Antiviral Research 212 (2023) 105568

Contents lists available at ScienceDirect

Antiviral Research

journal homepage: www.elsevier.com/locate/antiviral

Identification of West Nile virus RNA-dependent RNA polymerase non-nucleoside inhibitors by real-time high throughput fluorescence screening

Marta García-Zarandieta [a], Ernesto Quesada [b], María I. Martínez-Jiménez [c], Cristina V. Newnes [a], Victor Fernández-Cabello [b], Yanira Sáez-Álvarez [a], Ana-Belén Blázquez [d], Estela Escribano-Romero [d], Juan-Carlos Saiz [d], Carmen Del Aguila [a], Miguel A. Martín-Acebes [d], María-Jesús Pérez-Pérez [b], Rubén Agudo [a,*]

[a] Facultad de Farmacia, Universidad San Pablo-CEU, CEU Universities, Urbanización Montepríncipe, 28660, Boadilla del Monte, Spain
[b] Instituto de Química Médica (IQM, CSIC), 28006, Madrid, Spain
[c] Centro de Biología Molecular 'Severo Ochoa' (CSIC-UAM), Cantoblanco, E-28049, Madrid, Spain
[d] Departamento de Biotecnología, Instituto Nacional de Investigación y Tecnología Agraria y Alimentaria, (INIA, CSIC), 289040, Madrid, Spain

ARTICLE INFO

Keywords:
West nile virus
Antiviral
Rilpivirine
Nonnucleoside analogues
NS5
RNA-Dependent RNA polymerase

ABSTRACT

West Nile virus (WNV) is a re-emergent mosquito-borne RNA virus that causes major outbreaks of encephalitis around the world. However, there is no therapeutic treatment to struggle against WNV, and the current treatment relies on alleviating symptoms. Therefore, due to the threat virus poses to animal and human health, there is an urgent need to come up with fast strategies to identify and assess effective antiviral compounds. A relevant target when developing drugs against RNA viruses is the viral RNA-dependent RNA polymerase (RdRp), responsible for the replication of the viral genome within a host cell. RdRps are key therapeutic targets based on their specificity for RNA and their essential role in the propagation of the infection. We have developed a fluorescence-based method to measure WNV RdRp activity in a fast and reliable real-time way. Interestingly, rilpivirine has shown in our assay inhibition of the WNV RdRp activity with an IC_{50} value of 3.3 μM and its antiviral activity was confirmed in cell cultures. Furthermore, this method has been extended to build up a high-throughput screening platform to identify WNV polymerase inhibitors. By screening a small chemical library, novel RdRp inhibitors **1–4** have been identified. When their antiviral activity was tested against WNV in cell culture, **4** exhibited an EC_{50} value of 2.5 μM and a selective index of 12.3. *Thus, rilpivirine shows up as an interesting candidate for repurposing against flavivirus. Moreover, the here reported method allows the rapid identification of new WNV RdRp inhibitors.*

1. Introduction

The genus *Flavivirus* encompasses a wide range of well-known pathogenic viruses such as Dengue Virus (DENV), Zika Virus (ZIKV), Yellow Fever Virus (YFV), Japanese Encephalitis Virus (JEV), Tick-borne encephalitis Virus (TBEV) or West Nile Virus (WNV). These arthropod-borne viruses (arboviruses) cause hemorrhagic fevers, encephalitis, teratogenic problems in fetuses or other neurological disorders (Barrows et al., 2018). In the case of WNV, the bite of infected mosquitos can cause a febrile illness and severe neurological diseases, including meningitis, encephalitis, and acute flaccid paralysis (David and Abraham, 2016).

WNV virions (50 nm in diameter) contain a positive single-stranded genomic RNA of 11 kb. This genome encodes a single polyprotein, which is processed into three structural proteins (capsid, membrane, and envelope), and seven nonstructural proteins (NS1, NS2A, NS2B, NS3, NS4A, NS4B, and NS5). The NS5 protein is the main actor in the replication and transcription viral processes. The N-terminal domain of this protein (amino acids 1–272) contains the methyltransferase activity, responsible for generating the cap structure at the 5′ end of newly synthesized RNA (Issur et al., 2009; Ray et al., 2006), that promotes the translation (Fajardo et al., 2020; Zhou et al., 2007) and is involved in the

* Corresponding author.
E-mail address: ruben.agudotorres@ceu.es (R. Agudo).

https://doi.org/10.1016/j.antiviral.2023.105568
Received 25 November 2022; Received in revised form 20 February 2023; Accepted 21 February 2023
Available online 24 February 2023

evasion of the host's innate immune response (Daffis et al., 2010; Fleith et al., 2018). The RNA-dependent RNA polymerase (RdRp) activity is located at the C-terminal domain (Barrows et al., 2018) of NS5 (amino acids 273–905) and is responsible for viral genome transcription and replication, which starts by a *de novo* mechanism, the hallmark activity of flavivirus RdRps (Selisko et al., 2006). The three-dimensional structure of the two WNV NS5 motives has been solved separately (Malet et al., 2007; Zhou et al., 2007). They share similar architecture and conserved motifs as those observed in the structure of full-length flavivirus NS5 proteins (Lu and Gong, 2013; Zhao et al., 2015, 2017). The WNV RdRp domain possess the right hand-like typical structure of nucleic acid polymerases containing fingers, palm and thumb subdomains (Lu and Gong, 2017; Malet et al., 2007). Within these subdomains are the crucial motifs involved in both RNA and nucleotide binding and the key residues for the nucleotidyl transfer reaction which endow NS5 with RdRp activity (Lu and Gong, 2017; Malet et al., 2007; Wu et al., 2015). Thus, the fundamental role of RdRp in the virus replicative cycle makes it an excellent target for direct-acting antiviral drugs (Dong et al., 2008; Malet et al., 2008). Depending on their chemical structure, two main classes of RdRp inhibitors have been described: nucleoside or nonnucleoside analogues (NAs or NNAs, respectively). NAs are prodrugs that after activation mimic the natural polymerase substrates, and are incorporated in the nascent RNA strain, leading to chain-termination (Eyer et al., 2018) and/or lethal mutagenesis (Perales et al., 2011). On the contrary, NNAs bind to allosteric sites outside the catalytic site, inducing conformational changes that lead to inhibition of the polymerase activity (Acharya and Bai, 2016; Sinokrot et al., 2017). The effect of NAs on WNV RdRp domain has been studied both *in vivo* and in *vitro*, but the results obtained have not progressed to the identification of a clinical candidate (Saiz et al., 2021). This highlights the pressing need to identify new candidates that, by targeting NS5 RdRp activity, may lead to new drugs to control WNV infection.

In this study, we have used a high throughput fluorescence-based activity assay to measure the RdRp activity of WNV NS5. Using our method, we have demonstrated that the antiviral rilpivirine impedes the WNV NS5 RdRp activity. Moreover, the prospectiveness of the assay is exemplified by identifying WNV NS5 polymerase activity inhibitors after sampling a small chemical library of compounds without previously known antiviral activity. In addition to rilpivirine, we have also identified novel compounds that displayed good antiviral profiles in terms of activity and selectivity when tested in cell culture assays against WNV.

2. Materials and Methods

2.1. Reagents and hit compounds

A comprehensive list of reagents used in this study, as well as the synthesis and structural characterization of the hit compounds **1**–**4** are included in the supplementary material.

2.2. Radioactivity-based polymerization assay

Standard radioactivity assays were performed in 20 μL reactions containing 50 mM Tris-HCl, pH 7.5, 2.5 mM $MnCl_2$, 0.1 mg/mL BSA, 5 mM DTT, 500 μM ATP, 16 nM [α-^{32}P]ATP and 20 ng of poly-U. After starting the reactions by addition of NS5 WNV (950 nM), samples were incubated at 30 °C for the indicated time. Samples were stopped by the addition of 8 μL of loading buffer [10 mM EDTA, 95% (v/v) formamide, 0.03% (w/v), xylene-cyanol]. The reaction products were incubated at 85 °C for 5 min and then loaded onto 12.5% polyacrylamide, 8M urea gels. After electrophoresis (50W for 120 min in 1X TBE buffer), the *de novo* polymerization products were detected by autoradiography. Different variations of this protocol are properly indicated in the legend of Fig. 1.

2.3. Activity in the presence of inhibitory compounds

Assays were performed using a 96-well plate format, each well contained 0.5 μL of each compound (5 mM in DMSO) and starting the polymerization reaction by addition of 49.5 μL of reaction mix (50 mM Tris-HCl, pH 7.5, 2.5 mM MnCl2, 500 μM ATP, 5 mM DTT, 1 ng/μL poly-U, 0.1 mg/mL BSA, 0.25 μM SYTO-9, and 300 nM of recombinant WNV NS5) with a multichannel micropipette to streamline the filling process. The half-maximal inhibitory concentrations (IC_{50}) were calculated performing fluorescence-based polymerization assays using increasing concentrations of the inhibitory compounds. The determination of the mechanism of inhibition was carried out using variable concentrations of ATP (200–800 μM) with increasing amounts of inhibitor. Relative velocity data were represented by Lineweaver-Burk plots. In all cases, the activity values were determined as the velocity of polymerization recorded from minute 7 to minute 10 of the reaction. Statistical and data analysis data treatment is explained in the supplementary material.

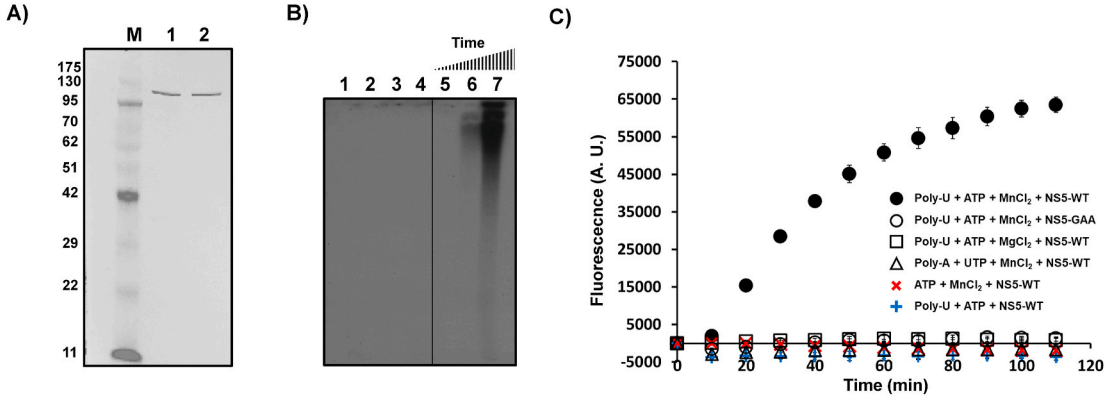

Fig. 1. Purification and activity of WNV NS5. A) SDS-PAGE analysis of WNV NS5 protein expressed in *E. coli* BL21 (DE3)-pRIL and purified by affinity chromatography. NS5-WT (lane 1) and NS5-GAA (lane 2) recombinant proteins after purification by Ni-NTA resin. M, molecular weight marker. Molecular weight (in kDa) of each standard band is indicated. B) Representative electrophoretic analysis of control polymerization reactions conducted in the absence of NS5-WT (lane 1), poly-U (lane 2), ATP (lane 3), or using NS5-GAA (lane 4). Standard reactions carried out by WNV NS5 as described in Section 3.4 reactions were stopped at increasing time points (15, 30 and 60 min, lanes 5 to 7, respectively). C) Polymerization assay measured by fluorescence in the presence of the indicated reagents, keeping the rest of experimental conditions as in a preliminary assay (Materials and Methods). Emission kinetics was recorded during 110 min, measuring the fluorescence each 30 s. The experiments were performed in quintuplicate.

2.4. Infections and drug treatments

Infectious virus manipulations were conducted in biosafety level 3 facilities. The origin of lineage 2 WNV Novi Sad/12 (Genebank accession: KC407673.1) isolate has been previously described (Petrovic et al., 2013). All infections were performed on Vero CCL-81 cells (ATTC). Cells were infected (MOI of 1) and viral inoculum was removed after 1 h of adsorption and replaced by fresh medium containing the compounds or drug vehicle (DMSO). WNV titers were determined 24 h postinfection (p.i.) by standard plaque assay is semisolid agarose medium (Martin-Acebes and Saiz, 2011; Merino-Ramos et al., 2016). At this time post-infection titers in control samples were in the range of 10^8 PFU/mL. Cellular ATP content was measured to monitor cell viability in uninfected cells using the Cell Titer Glo luminescent cell viability assay.

2.5. Statistical and data analysis

Fluorometric results were expressed as mean ± SD, indicating in each case, the number of experimental replicates. Dose-response and Lineweaver-Burk plots were obtained from non-linear regression curve fitting. Nonlinear regression was determined using GraphPad Prism 9 program. Z′ factor value was calculated as statistical estimator to evaluate the suitability of a prospective method as a high-throughput system (Zhang et al., 1999). This factor was calculated as previously described (Saez-Alvarez et al., 2019): $Z' = 1 - [(3SD_{c+} + 3SD_{c-})/(mean_{c+} - mean_{c-})]$ where "c+" is the activity obtained in a standard assay and "c−" is the activity obtained in a negative assay in the absence of $MnCl_2$.

3. Result

3.1. Purification and biochemical characterization of recombinant WNV NS5

NS5-WT and NS5-GAA (a catalytically inactive mutant of WNV NS5 RdRp domain, see supplementary material) recombinant proteins were expressed and purified as described in Section 2.2 (Fig. 1A), and a polymerization assay was carried out to check their activity. Reactions were performed using only [α-^{32}P]ATP and poly-U as substrates, and the polymerization products were dissolved on a polyacrylamide gel. RNA synthesis was observed only when NS5-WT was used in addition of both template and $MnCl_2$ (Fig. 1B). This result agrees with previous results, confirming that, in the presence of Mn^{2+}, homopolymeric ssRNA can be used as template for *de novo* polymerization carried out by flavivirus RdRps (Saez-Alvarez et al., 2019; Selisko et al., 2006). This result encouraged us to build up a fast non-radioactive assay for screening compounds as inhibitors of the polymerase activity of WNV NS5, based on our previously reported real-time polymerization method (Agudo et al., 2017; Saez-Alvarez et al., 2019). This technique relies on the strong binding preference of fluorescent dye SYTO-9 towards dsRNA versus ssRNA, so that the dye will bind to nascent dsRNA synthesized by WNV NS5 during the assay. The real-time increase of fluorescence was only detected in assays carried out in the presence poly-U and $MnCl_2$ using NS5-WT. The same assay conditions using the mutant NS5-GAA provided identical results, confirming the importance of the catalytic activity of RdRp for detecting increase fluorescence (Fig. 1C). In addition, no NS5 fluorescence-associated activity was shown when the substrates were poly-A and UTP, or when Mg^{2+} was used as a metal donor.

Several parameters were explored to optimize the fluorescence assay. Different concentrations of the metal donor, NaCl, DTT and of the recombinant protein, as well as different temperatures, were tested while the rest of the experimental conditions remained unaltered. The best results (Supplementary Fig. 1) were obtained using 2.5 mM $MnCl_2$, in the absence of additional NaCl, 10 mM DTT and the temperature fixed at 25 °C. As expected, no increase in fluorescence was detected under the range of $MgCl_2$ concentrations used (0–10 mM). The increment of the reaction velocity is directly proportional to the concentration of the recombinant NS5 in the 200–600 nM range, reaching its maximum when 1250 nM of recombinant protein was used (Supplementary Fig. 1). These assays allowed the determination of a K_m for poly-U of 2.2 ± 0.8 μg/mL (~21 nM) and a K_m for ATP of 204 ± 55 μM (Supplementary Fig. 2).

3.2. Utility of the fluorescence assay to evaluate the effect of polymerase inhibitors

Based on our previous experience (Saez-Alvarez et al., 2021), we considered that the WNV NS5 fluorescence-based polymerization assay might be exploited as a high-throughput platform for the screening of potential inhibitors of RdRp activity. Towards this aim, we carried out fluorescence-based experiments in the presence of cordycepin 5′-triphosphate (3′-dATP; Fig. 2A), a model compound acting as a chain terminator analog of ATP (Rose et al., 1977), which has been proven as polymerization inhibitor for several Flaviviridal RdRps (Ackermann and Padmanabhan, 2001; Lu et al., 2017; Nomaguchi et al., 2004) The presence of 3′-dATP resulted in a concentration-dependent reduction of the fluorescence. The IC_{50} value of 3′-dATP was 60.8 ± 7.8 μM (Fig. 2B). Radioactive-based polymerization assays confirmed that the inhibitory activity elicited by 3′-dATP was related to the inhibition of dsRNA synthesis (Fig. 2C).

To further assess the suitability of the fluorescence assay as a high-throughput screening method, the Z′ value was determined. The relative activity of both positive and negative controls was calculated as the average value obtained from ten independent experiments. Each experiment was carried out in triplicate and on independent days. The Z' value obtained was 0.65. According to published standards (Zhang et al., 1999), this result qualifies our method as an excellent assay for high-throughput screening applications.

3.3. Rilpivirine inhibits WNV RdRp activity

Recently, rilpivirine (Fig. 3A), an antiretroviral targeting the human immunodeficiency virus reverse transcriptase acting as a NNA (Janssen et al., 2005), has been proposed to bind ZIKV NS5 polymerase at the palm domain (Sariyer et al., 2019). Rilpivirine showed anti-ZIKV activity in primary astrocytes and prevented ZIKV-induced mortality in a mice model (Sariyer et al., 2019). Thus, rilpivirine was selected as a potential inhibitor of WNV polymerase to be tested in the here reported fluorescence-based assay. Indeed, rilpivirine showed a strong dose-dependent inhibition of NS5-WT activity, showing an $IC_{50} = 3.3 \pm 0.5$ μM (Fig. 3B). Also in this case, radioactive-based polymerization assays confirmed that synthesis of RNA by NS5-WT was inhibited by rilpivirine (Fig. 3C). To the best of our knowledge this is the first report on WNV RdRp inhibition by rilpivirine.

3.4. Identification of potential WNV NS5 inhibitors through fluorescence-based screening

To assess the usefulness of the screening platform, it was challenged by analyzing a small in-house chemical library that contains 120 compounds with MW < 500. The screening of this library was performed as a proof of concept to evaluate a source of chemicals without known antiviral activity. The library was tested at a final concentration of 100 μM. Only four compounds **1**–**4** (Fig. 4) afforded complete inhibition of the fluorescent signal compared to a control containing DMSO, so they were considered *hits*. The IC_{50} values for **1**, **2**, **3** and **4** were determined as 9.8 ± 0.7 μM, 7.8 ± 0.7 μM, 9.8 ± 0.5 μM and 12.4 ± 2.5 μM, respectively (Fig. 4). All compounds showed non-competitive inhibition versus ATP according to Lineweaver-Burk plots (Fig. 5).

All together, these results show the high potential of the fluorescence-based method for the identification and biochemical characterization of novel antiviral agents against WNV.

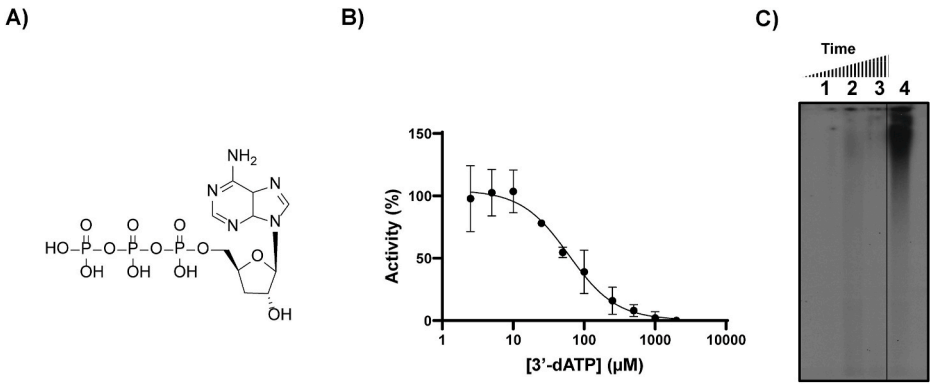

Fig. 2. Enzymatic activity of NS5-WT in the presence of model inhibitory compounds. A) Chemical structure of 3′dATP. B) Dose-response curve of NS5-WT in the presence of 3′-dATP used as model inhibitory compound. The experiments were performed in quadruplicate. C) Representative electropherogram of standard radioactive assay performed with NS5-WT in the presence of 50 μM 3′-dATP stopped at 15′, 30′ and 60′ minutes (lanes 1 to 3, respectively). A positive control reaction stopped at 60′ in the absence of 3′-dATP is shown for comparison, (lane 4).

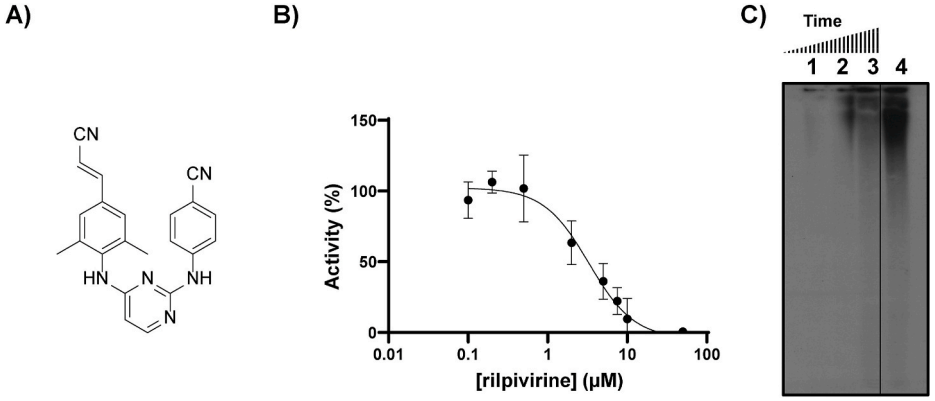

Fig. 3. Enzymatic activity of NS5-WT in the presence of rilpivirine. A) Chemical structure of rilpivirine. B) Concentration-response curve of NS5-WT in the presence of rilpivirine used as model inhibitory compound. The experiments were performed in quadruplicate. C) Representative electropherogram of standard radioactive assay performed with NS5-WT in the presence of 10 μM rilpivirine stopped at 15′, 30′ and 60′ minutes (lanes 1 to 3, respectively). A positive control reaction stopped at 60′ in the absence of rilpivirine is shown for comparison (lane 4).

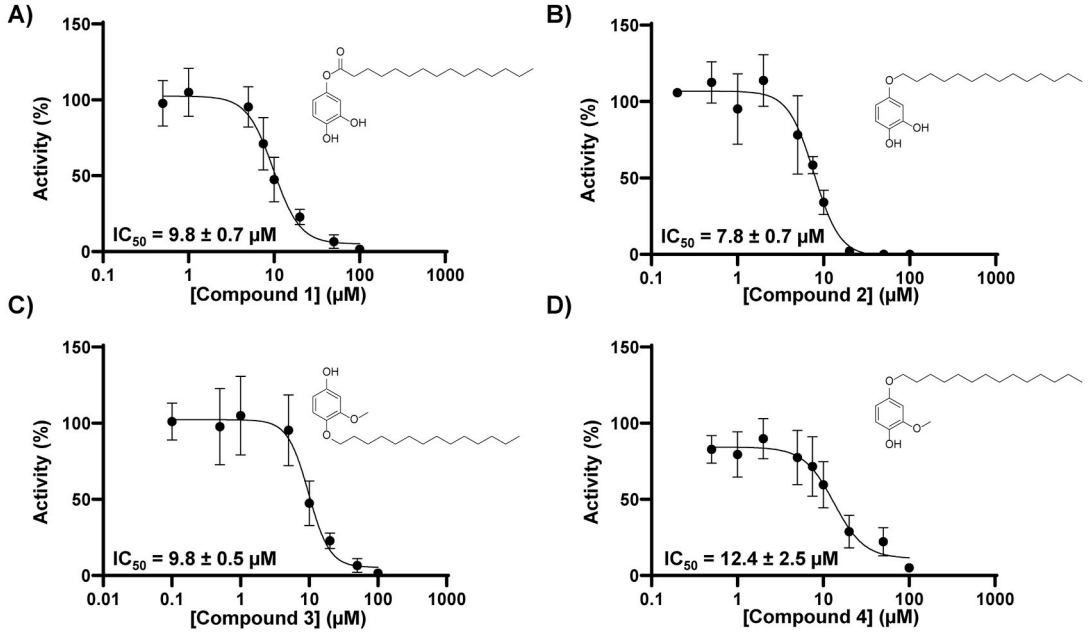

Fig. 4. Dose-response inhibition of the RdRp activity *in vitro* of WNV NS5 exerted by hit compounds 1–4. A) Chemical structure and IC_{50} calculation of compound **1** B) Chemical structure and IC_{50} calculation of compound **2.** C) Chemical structure and IC_{50} calculation of compound **3.** D) Chemical structure and IC_{50} calculation of compound **4**.

3.5. Antiviral activity against WNV in cell culture assays

In order to assess the antiviral activity of rilpivirine and the here identified NS5 polymerase inhibitors **1–4** against WNV, cell culture assays were performed in Vero cells (Fig. 6). Rilpivirine exhibited good antiviral activity against WNV in these assays with EC_{50} of 1.5 μM and low cytotoxicity (CC_{50} > 100 μM), thus accounting for a Selectivity Index (SI; calculated as the ratio CC_{50}/EC_{50}) of 66.6 (Fig. 6A). Regarding

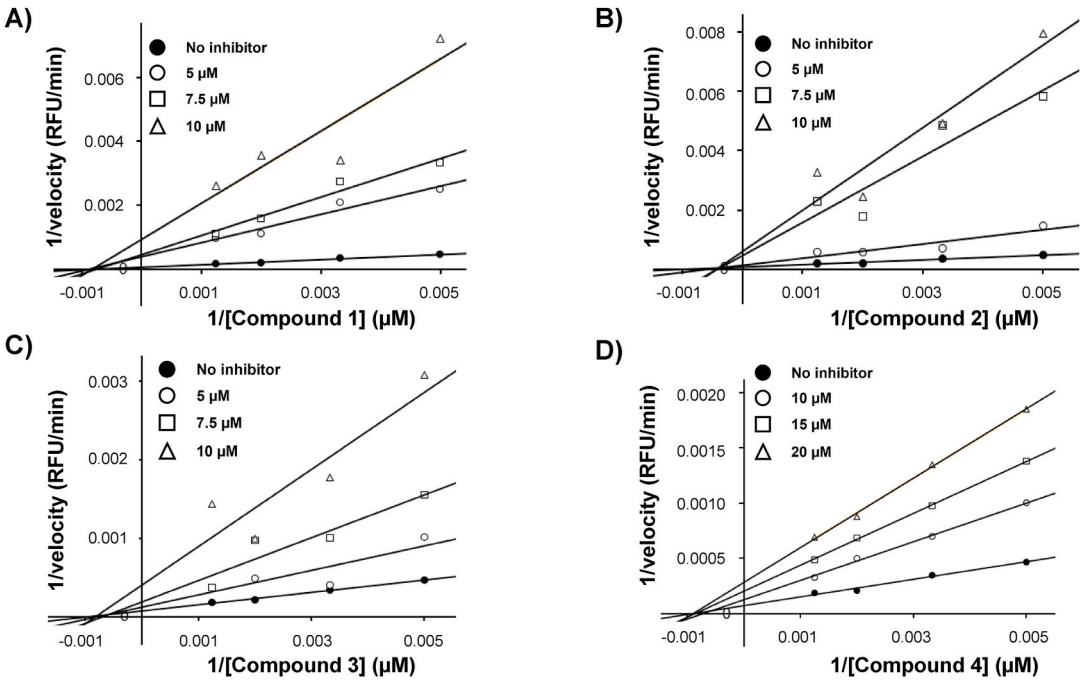

Fig. 5. Characterization of inhibition exerted by hit compounds 1–4. A to D) Kinetics of polymerization inhibition by hit compounds **1**, **2**, **3** and **4**. Lineweaver–Burk plot of the polymerization catalyzed by NS5-WT in the absence, or in the presence of the indicated amounts of each compound.

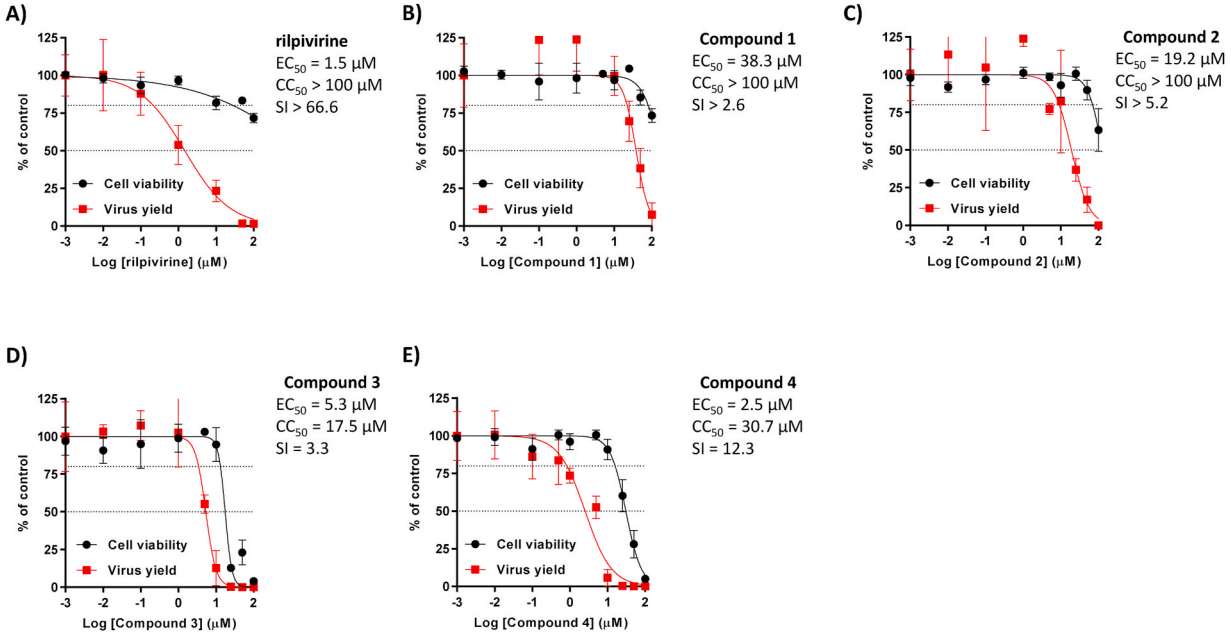

Fig. 6. Antiviral activity of rilpivirine and compounds 1–4 against WNV. A) to E) EC_{50} and CC_{50} calculations of rilpivirine (A) and compounds **1** (B), **2** (C), **3** (D) and **4** (E). Vero cells were inoculated with WNV (MOI of 1), treated with the compounds and the virus yield was determined a 24 h post-infection. The cytotoxicity was measured in parallel in uninfected cells treated with the same amounts of the compounds by quantification of ATP levels. 50% and 80% are denoted by dashed lines. At least three independent biological replicates were performed.

the identified hits **1–4**, compound **1** showed almost no activity against WNV replication (EC_{50} of 38.3 μM) (Fig. 6B). This lack of activity may be ascribed to the potential hydrolysis of the labile ester bond linking the palmitic fatty acid to the aromatic core. Remarkably, its non-hydrolysable ether analogue **2** showed an improved activity (EC_{50} of 21 μM) in the absence of toxicity (CC_{50} > 100 μM) (Fig. 6C). More interestingly, the ether derivative **3** exhibited an EC_{50} value of 5.3 μM although toxicity was also observed with a CC_{50} of 17.5 μM (Fig. 6D). The best compound in this series is compound **4**, with an EC_{50} value of 2.5 μM and a CC_{50} of 30.7 μM, thus affording a selectivity index of 12.3 (Fig. 6E). Compounds **1** to **3** exhibited SIs from 2.6 to 5.2 in cell cultures, so their antiviral activity was very close to the concentrations that started cytotoxicity (note 80% of viability in the graphs). Therefore, we cannot exclude that this activity could derive in part from cytotoxicity. However, in the case of compound **4** the SI > 10 supported its specificity. Overall, these results confirm the utility of the screening assay here developed to identify NS5 inhibitors with potential antiviral activity.

4. Discussion

The unique RNA-dependent RNA synthesis of RdRps, without known polymerase counterparts among living beings, convert those proteins in one of the main therapeutic targets against the RNA viruses. The crucial role of this enzyme in flavivirus replication has been evidenced by the antiviral activity of different NAs acting at the active site. Relevant examples described for WNV polymerase includes sofosbuvir (Dragoni et al., 2020), favipiravir (Escribano-Romero et al., 2017; Morrey et al., 2008), remdesivir (Konkolova et al., 2020), 7-deaza-2'-C-methyladenosine (Eyer et al., 2019), ribavirin (Anderson and Rahal, 2002) or 7-deaza-2'-C-ethynyladenosine (Nelson et al., 2015), which have produced varying degree of success. However, there is no compound found to be effective beyond *in vitro* models (Eyer et al., 2018), showing the need to develop new assays for antiviral compound screening.

The most ambitious campaign to identify non-nucleoside inhibitors of flavivirus NS5 has been performed with DENV RdRp by fragment identification using X-Ray crystallography (Noble et al., 2016), followed by ligand construction using structure-based drug design (Yokokawa et al., 2016) and additional studies on their mechanism of action and resistance profiling (Lim et al., 2016). These ligands have also been studied and further modified for ZIKV NS5 (Gharbi-Ayachi et al., 2020). To the best of our knowledge, this approach has not been applied to WNV NS5 and just a few examples have been described of non-nucleoside inhibitors against this protein (Puig-Basagoiti et al., 2009; Tarantino et al., 2016). Thus, there is really a lack of NNAs that show inhibitory activity targeting WNV NS5 RdRp.

Since our description of the capabilities of real-time fluorescence to measure the *de-novo* RNA synthesis using ZIKV RdRp (Saez-Alvarez et al., 2019), different authors have used variation of this method to measure the activity of enterovirus 71 (Xu et al., 2020), SARS-CoV-2 (Yin et al., 2021), ZIKV (Fernandes et al., 2021; Saez-Alvarez et al., 2021) and DENV (Wang et al., 2022) RdRps in the presence of different polymerase inhibitors. The benefits of this measurement method are captured again in this work. The here described WNV fluorescence-based technique to measure the RdRp activity does not require the presence of radioactive substances, which involve additional biosafety measures, contention facilities and cumbersome experimental conditions (Gong et al., 2013; Madhvi et al., 2017; Su et al., 2010). In addition, this method uses homopolymeric RNA molecules as templates that are easily accessible. The possibility of real-time recording the RdRp activity increases the specificity of the fluorometric method, since it can be possible to check in real time those samples not showing an increase of fluorescence from the beginning of the assay. This setup speeds up the screening capabilities and allows the calculation of the 96 reactions velocities of the plate analyzed in only 10 min, as described in Section 2.3. Data presented here shows that both standard radioactive- and fluorescence-based assay requirements are similar, including the presence of a catalytically active polymerase to obtain either a radiolabeled or fluorescent product, respectively (Fig. 1A and B). All these results support that our fluorescence-based method faithfully records the RdRp catalyzed RNA polymerization.

Fluorometric measurements in the presence or absence of 3′-dATP as a model of chain-terminator nucleotide analogue, revealed a positive correlation with the results obtained in the assay based on radiolabeled nucleotides (Fig. 2), thus this can be considered as a positive control. In a second step, we tested rilpivirine, an approved HIV-1 RT antiviral, which recently was reported to inhibit ZIKV replication by interfering with the NS5 polymerase (Sariyer et al., 2019). We have found that rilpivirine effectively inhibits WNV polymerase (Fig. 3) Moreover, rilpivirine showed a marked antiviral effect against WNV in cell culture with a SI > 66 (Fig. 6), data that, together with those reported for ZIKV, convert rilpivirine into a promising broad-spectrum anti-flaviviral compound.

The 96-well plate configuration and the high reproducibility allows using our fluorescence assay as a high-throughput screening (HTS) platform. The value obtained for factor Z' (0.65) qualifies this method as an HTS platform of inhibitory compounds targeting the WNV RdRp activity. As proof of concept of the platform capacity, a small chemical library composed of molecules without known antiviral activity was screened. Four structurally related compounds (**1**–**4**, Fig. 4) were identified as inhibitors of the polymerase reaction with IC_{50} values in the low micromolar range, and in all cases, they proved to be ATP-non-competitive inhibitors in the fluorescence assay (Fig. 5), suggesting their binding to an allosteric pocket outside the active site of the polymerase. Although, to the best of our knowledge, no information is available on crystal structures of allosteric inhibitors binding to the WNV polymerase domain, the existence of allosteric pockets for this enzyme has been suggested based on sequence analysis comparison with other flavivirus RdRps, both at the so called N-pocket (Noble et al., 2016) or, more recently, to the RNA template tunnel (Arora et al., 2020).

Concerning the antiviral effect against WNV in cell culture, two of these compounds (**3** and **4**) showed EC_{50} values lower than 10 μM against WNV (Fig. 6). Particularly interesting is compound **4**, with marked antiviral activity (EC_{50} of 2.5 μM) and a good selectivity index of 12, making of this compound a good prototype for the development of novel NNAs directed against WNV polymerase.

5. Conclusions

In this work we have set-up a real-time HTS platform to measure the WNV RdRp activity that can be of special relevance to the discovery, characterization and development of therapeutics against WNV which are currently unavailable. The inhibitory activity of rilpivirine against WNV RdRp, together with the identification of a novel inhibitor of this enzyme (i.e. compound **4**) both of them antivirally active in cell culture, open new possibilities for the future development therapeutics to combat this pathogen.

Declaration of competing interest

The authors declare that they have no known competing financial interests or personal relationships that could have appeared to influence the work reported in this paper.

Data availability

Data will be made available on request.

Acknowledgements

This work was supported by Spanish Ministry of Science and Innovation AEI/10.13039/501100011033 under grant PID2020-115432RB-I00 (to R.A) grant PID2019-105117RR-C21 (to MAM-A); PID2019-105117RR-C22 (to M-JP-P); and from AECSIC under grant PIE-201980E100 (to M-JP-P). This research work was also funded by the European Commission-NextGeneration EU (Regulation EU 2020/2094), through CSIC's Global Health Platform (PTI Salud Global).

Appendix A. Supplementary data

Supplementary data to this article can be found online at https://doi.org/10.1016/j.antiviral.2023.105568.

References

Ackermann, M., Padmanabhan, R., 2001. De novo synthesis of RNA by the dengue virus RNA-dependent RNA polymerase exhibits temperature dependence at the initiation but not elongation phase. J. Biol. Chem. 276, 39926–39937.

Acharya, D., Bai, F., 2016. An overview of current approaches toward the treatment and prevention of West Nile virus infection. Methods Mol. Biol. 1435, 249–291.

Agudo, R., Calvo, P.A., Martinez-Jimenez, M.I., Blanco, L., 2017. Engineering human PrimPol into an efficient RNA-dependent-DNA primase/polymerase. Nucleic Acids Res. 45, 9046–9058.
Anderson, J.F., Rahal, J.J., 2002. Efficacy of interferon alpha-2b and ribavirin against West Nile virus in vitro. Emerg. Infect. Dis. 8, 107–108.
Arora, R., Liew, C.W., Soh, T.S., Otoo, D.A., Seh, C.C., Yue, K., Nilar, S., Wang, G., Yokokawa, F., Noble, C.G., Chen, Y.L., Shi, P.Y., Lescar, J., Smith, T.M., Benson, T.E., Lim, S.P., 2020. Two RNA tunnel inhibitors bind in highly conserved sites in dengue virus NS5 polymerase: structural and functional studies. J. Virol. 94.
Barrows, N.J., Campos, R.K., Liao, K.C., Prasanth, K.R., Soto-Acosta, R., Yeh, S.C., Schott-Lerner, G., Pompon, J., Sessions, O.M., Bradrick, S.S., Garcia-Blanco, M.A., 2018. Biochemistry and molecular biology of flaviviruses. Chem. Rev. 118, 4448–4482.
Daffis, S., Szretter, K.J., Schriewer, J., Li, J., Youn, S., Errett, J., Lin, T.Y., Schneller, S., Zust, R., Dong, H., Thiel, V., Sen, G.C., Fensterl, V., Klimstra, W.B., Pierson, T.C., Buller, R.M., Gale Jr., M., Shi, P.Y., Diamond, M.S., 2010. 2'-O methylation of the viral mRNA cap evades host restriction by IFIT family members. Nature 468, 452–456.
David, S., Abraham, A.M., 2016. Epidemiological and clinical aspects on West Nile virus, a globally emerging pathogen. Infectious diseases 48, 571–586.
Dong, H., Zhang, B., Shi, P.Y., 2008. Flavivirus methyltransferase: a novel antiviral target. Antivir. Res. 80, 1–10.
Dragoni, F., Boccuto, A., Picarazzi, F., Giannini, A., Giammarino, F., Saladini, F., Mori, M., Mastrangelo, E., Zazzi, M., Vicenti, I., 2020. Evaluation of sofosbuvir activity and resistance profile against West Nile virus in vitro. Antivir. Res. 175, 104708.
Escribano-Romero, E., Jimenez de Oya, N., Domingo, E., Saiz, J.C., 2017. Extinction of West Nile virus by favipiravir through lethal mutagenesis. Antimicrob. Agents Chemother. 61.
Eyer, L., Fojtikova, M., Nencka, R., Rudolf, I., Hubalek, Z., Ruzek, D., 2019. Viral RNA-dependent RNA polymerase inhibitor 7-deaza-2'-C-methyladenosine prevents death in a mouse model of West Nile virus infection. Antimicrob. Agents Chemother. 63.
Eyer, L., Nencka, R., de Clercq, E., Seley-Radtke, K., Ruzek, D., 2018. Nucleoside analogs as a rich source of antiviral agents active against arthropod-borne flaviviruses. Antivir. Chem. Chemother. 26, 2040206618761299.
Fajardo, T., Sanford, T.J., Mears, H.V., Jasper, A., Storrie, S., Mansur, D.S., Sweeney, T. R., 2020. The flavivirus polymerase NS5 regulates translation of viral genomic RNA. Nucleic Acids Res. 48, 5081–5093.
Fernandes, R.S., de Godoy, A.S., Santos, I.A., Noske, G.D., de Oliveira, K.I.Z., Gawriljuk, V.O., Gomes Jardim, A.C., Oliva, G., 2021. Discovery of an imidazonaphthyridine and a riminophenazine as potent anti-Zika virus agents through a replicon-based high-throughput screening. Virus Res. 299, 198388.
Fleith, R.C., Mears, H.V., Leong, X.Y., Sanford, T.J., Emmott, E., Graham, S.C., Mansur, D.S., Sweeney, T.R., 2018. IFIT3 and IFIT2/3 promote IFIT1-mediated translation inhibition by enhancing binding to non-self RNA. Nucleic Acids Res. 46, 5269–5285.
Gharbi-Ayachi, A., Santhanakrishnan, S., Wong, Y.H., Chan, K.W.K., Tan, S.T., Bates, R. W., Vasudevan, S.G., El Sahili, A., Lescar, J., 2020. Non-nucleoside inhibitors of Zika virus RNA-dependent RNA polymerase. J. Virol. 94.
Gong, E.Y., Kenens, H., Ivens, T., Dockx, K., Vermeiren, K., Vandercruyssen, G., Devogelaere, B., Lory, P., Kraus, G., 2013. Expression and purification of dengue virus NS5 polymerase and development of a high-throughput enzymatic assay for screening inhibitors of dengue polymerase. Methods Mol. Biol. 1030, 237–247.
Issur, M., Geiss, B.J., Bougie, I., Picard-Jean, F., Despins, S., Mayette, J., Hobdey, S.E., Bisaillon, M., 2009. The flavivirus NS5 protein is a true RNA guanylyltransferase that catalyzes a two-step reaction to form the RNA cap structure. RNA 15, 2340–2350.
Janssen, P.A., Lewi, P.J., Arnold, E., Daeyaert, F., de Jonge, M., Heeres, J., Koymans, L., Vinkers, M., Guillemont, J., Pasquier, E., Kukla, M., Ludovici, D., Andries, K., de Bethune, M.P., Pauwels, R., Das, K., Clark Jr., A.D., Frenkel, Y.V., Hughes, S.H., Medaer, B., De Knaep, F., Bohets, H., De Clerck, F., Lampo, A., Williams, P., Stoffels, P., 2005. In search of a novel anti-HIV drug: multidisciplinary coordination in the discovery of 4-[[4-[[4-[(1E)-2-cyanoethenyl]-2,6-dimethylphenyl]amino]-2-pyrimidinyl]amino]benzonitrile (R278474, rilpivirine). J. Med. Chem. 48, 1901–1909.
Konkolova, E., Dejmek, M., Hrebabecky, H., Sala, M., Boserle, J., Nencka, R., Boura, E., 2020. Remdesivir triphosphate can efficiently inhibit the RNA-dependent RNA polymerase from various flaviviruses. Antivir. Res. 182, 104899.
Lim, S.P., Noble, C.G., Seh, C.C., Soh, T.S., El Sahili, A., Chan, G.K., Lescar, J., Arora, R., Benson, T., Nilar, S., Manjunatha, U., Wan, K.F., Dong, H., Xie, X., Shi, P.Y., Yokokawa, F., 2016. Potent allosteric dengue virus NS5 polymerase inhibitors: mechanism of action and resistance profiling. PLoS Pathog. 12, e1005737.
Lu, G., Bluemling, G.R., Collop, P., Hager, M., Kuiper, D., Gurale, B.P., Painter, G.R., De La Rosa, A., Kolykhalov, A.A., 2017. Analysis of ribonucleotide 5'-triphosphate analogs as potential inhibitors of Zika virus RNA-dependent RNA polymerase by using nonradioactive polymerase assays. Antimicrob. Agents Chemother. 61.
Lu, G., Gong, P., 2013. Crystal Structure of the full-length Japanese encephalitis virus NS5 reveals a conserved methyltransferase-polymerase interface. PLoS Pathog. 9, e1003549.
Lu, G., Gong, P., 2017. A structural view of the RNA-dependent RNA polymerases from the Flavivirus genus. Virus Res. 234, 34–43.
Madhvi, A., Hingane, S., Srivastav, R., Joshi, N., Subramani, C., Muthumohan, R., Khasa, R., Varshney, S., Kalia, M., Vrati, S., Surjit, M., Ranjith-Kumar, C.T., 2017. A screen for novel hepatitis C virus RdRp inhibitor identifies a broad-spectrum antiviral compound. Sci. Rep. 7, 5816.
Malet, H., Egloff, M.P., Selisko, B., Butcher, R.E., Wright, P.J., Roberts, M., Gruez, A., Sulzenbacher, G., Vonrhein, C., Bricogne, G., Mackenzie, J.M., Khromykh, A.A., Davidson, A.D., Canard, B., 2007. Crystal structure of the RNA polymerase domain of the West Nile virus non-structural protein 5. J. Biol. Chem. 282, 10678–10689.
Malet, H., Masse, N., Selisko, B., Romette, J.L., Alvarez, K., Guillemot, J.C., Tolou, H., Yap, T.L., Vasudevan, S., Lescar, J., Canard, B., 2008. The flavivirus polymerase as a target for drug discovery. Antivir. Res. 80, 23–35.
Martin-Acebes, M.A., Saiz, J.C., 2011. A West Nile virus mutant with increased resistance to acid-induced inactivation. J. Gen. Virol. 92, 831–840.
Merino-Ramos, T., Vazquez-Calvo, A., Casas, J., Sobrino, F., Saiz, J.C., Martin-Acebes, M. A., 2016. Modification of the host cell lipid metabolism induced by hypolipidemic drugs targeting the acetyl coenzyme A carboxylase impairs West Nile virus replication. Antimicrob. Agents Chemother. 60, 307–315.
Morrey, J.D., Taro, B.S., Siddharthan, V., Wang, H., Smee, D.F., Christensen, A.J., Furuta, Y., 2008. Efficacy of orally administered T-705 pyrazine analog on lethal West Nile virus infection in rodents. Antivir. Res. 80, 377–379.
Nelson, J., Roe, K., Orillo, B., Shi, P.Y., Verma, S., 2015. Combined treatment of adenosine nucleoside inhibitor NITD008 and histone deacetylase inhibitor vorinostat represents an immunotherapy strategy to ameliorate West Nile virus infection. Antivir. Res. 122, 39–45.
Noble, C.G., Lim, S.P., Arora, R., Yokokawa, F., Nilar, S., Seh, C.C., Wright, S.K., Benson, T.E., Smith, P.W., Shi, P.Y., 2016. A conserved pocket in the dengue virus polymerase identified through fragment-based screening. J. Biol. Chem. 291, 8541–8548.
Nomaguchi, M., Teramoto, T., Yu, L., Markoff, L., Padmanabhan, R., 2004. Requirements for West Nile virus (-)- and (+)-strand subgenomic RNA synthesis in vitro by the viral RNA-dependent RNA polymerase expressed in Escherichia coli. J. Biol. Chem. 279, 12141–12151.
Perales, C., Martin, V., Domingo, E., 2011. Lethal mutagenesis of viruses. Current opinion in virology 1, 419–422.
Petrovic, T., Blazquez, A.B., Lupulovic, D., Lazic, G., Escribano-Romero, E., Fabijan, D., Kapetanov, M., Lazic, S., Saiz, J., 2013. Monitoring West Nile virus (WNV) infection in wild birds in Serbia during 2012: first isolation and characterisation of WNV strains from Serbia. Euro Surveill. : bulletin Europeen sur les maladies transmissibles = European communicable disease bulletin 18.
Puig-Basagoiti, F., Qing, M., Dong, H., Zhang, B., Zou, G., Yuan, Z., Shi, P.Y., 2009. Identification and characterization of inhibitors of West Nile virus. Antivir. Res. 83, 71–79.
Ray, D., Shah, A., Tilgner, M., Guo, Y., Zhao, Y., Dong, H., Deas, T.S., Zhou, Y., Li, H., Shi, P.Y., 2006. West Nile virus 5'-cap structure is formed by sequential guanine N-7 and ribose 2'-O methylations by nonstructural protein 5. J. Virol. 80, 8362–8370.
Rose, K.M., Bell, L.E., Jacob, S.T., 1977. Specific inhibition of chromatin-associated poly (A) synthesis in vitro by cordycepin 5'-triphosphate. Nature 267, 178–180.
Saez-Alvarez, Y., Arias, A., Del Aguila, C., Agudo, R., 2019. Development of a fluorescence-based method for the rapid determination of Zika virus polymerase activity and the screening of antiviral drugs. Sci. Rep. 9, 5397.
Saez-Alvarez, Y., Jimenez de Oya, N., Del Aguila, C., Saiz, J.C., Arias, A., Agudo, R., Martin-Acebes, M.A., 2021. Novel nonnucleoside inhibitors of Zika virus polymerase identified through the screening of an open library of antikinetoplastid compounds. Antimicrob. Agents Chemother. 65, e0089421.
Saiz, J.C., Martin-Acebes, M.A., Blazquez, A.B., Escribano-Romero, E., Poderoso, T., Jimenez de Oya, N., 2021. Pathogenicity and virulence of West Nile virus revisited eight decades after its first isolation. Virulence 12, 1145–1173.
Sariyer, I.K., Gordon, J., Burdo, T.H., Wollebo, H.S., Gianti, E., Donadoni, M., Bellizzi, A., Cicalese, S., Loomis, R., Robinson, J.A., Carnevale, V., Steiner, J., Ozdener, M.H., Miller, A.D., Amini, S., Klein, M.L., Khalili, K., 2019. Suppression of Zika virus infection in the brain by the antiretroviral drug rilpivirine. Mol. Ther. : the journal of the American Society of Gene Therapy 27, 2067–2079.
Selisko, B., Dutartre, H., Guillemot, J.C., Debarnot, C., Benarroch, D., Khromykh, A., Despres, P., Egloff, M.P., Canard, B., 2006. Comparative mechanistic studies of de novo RNA synthesis by flavivirus RNA-dependent RNA polymerases. Virology 351, 145–158.
Sinokrot, H., Smerat, T., Najjar, A., Karaman, R., 2017. Advanced prodrug strategies in nucleoside and non-nucleoside antiviral agents: a review of the recent five years. Molecules 22.
Su, C.Y., Cheng, T.J., Lin, M.I., Wang, S.Y., Huang, W.I., Lin-Chu, S.Y., Chen, Y.H., Wu, C. Y., Lai, M.M., Cheng, W.C., Wu, Y.T., Tsai, M.D., Cheng, Y.S., Wong, C.H., 2010. High-throughput identification of compounds targeting influenza RNA-dependent RNA polymerase activity. Proc. Natl. Acad. Sci. U. S. A 107, 19151–19156.
Tarantino, D., Cannalire, R., Mastrangelo, E., Croci, R., Querat, G., Barreca, M.L., Bolognesi, M., Manfroni, G., Cecchetti, V., Milani, M., 2016. Targeting flavivirus RNA dependent RNA polymerase through a pyridobenzothiazole inhibitor. Antivir. Res. 134, 226–235.
Wang, Z., Yan, Y., Dai, Q., Xu, Y., Yin, J., Li, W., Li, Y., Yang, X., Guo, X., Liu, M., Chen, X., Cao, R., Zhong, W., 2022. Azelnidipine Exhibits in Vitro and in Vivo Antiviral Effects against Flavivirus Infections by Targeting the Viral RdRp. Viruses 14.
Wu, J., Liu, W., Gong, P., 2015. A structural overview of RNA-dependent RNA polymerases from the flaviviridae family. Int. J. Mol. Sci. 16, 12943–12957.
Xu, N., Yang, J., Zheng, B., Zhang, Y., Cao, Y., Huan, C., Wang, S., Chang, J., Zhang, W., 2020. The pyrimidine analog FNC potently inhibits the replication of multiple enteroviruses. J. Virol. 94.
Yin, W., Luan, X., Li, Z., Zhou, Z., Wang, Q., Gao, M., Wang, X., Zhou, F., Shi, J., You, E., Liu, M., Wang, Q., Jiang, Y., Jiang, H., Xiao, G., Zhang, L., Yu, X., Zhang, S., Eric Xu, H., 2021. Structural basis for inhibition of the SARS-CoV-2 RNA polymerase by suramin. Nat. Struct. Mol. Biol. 28, 319–325.
Yokokawa, F., Nilar, S., Noble, C.G., Lim, S.P., Rao, R., Tania, S., Wang, G., Lee, G., Hunziker, J., Karuna, R., Manjunatha, U., Shi, P.Y., Smith, P.W., 2016. Discovery of

potent non-nucleoside inhibitors of dengue viral RNA-dependent RNA polymerase from a fragment hit using structure-based drug design. J. Med. Chem. 59, 3935–3952.

Zhang, J.H., Chung, T.D., Oldenburg, K.R., 1999. A simple statistical parameter for use in evaluation and validation of high throughput screening assays. J. Biomol. Screen 4, 67–73.

Zhao, B., Yi, G., Du, F., Chuang, Y.C., Vaughan, R.C., Sankaran, B., Kao, C.C., Li, P., 2017. Structure and function of the Zika virus full-length NS5 protein. Nat. Commun. 8, 14762.

Zhao, Y., Soh, T.S., Zheng, J., Chan, K.W., Phoo, W.W., Lee, C.C., Tay, M.Y., Swaminathan, K., Cornvik, T.C., Lim, S.P., Shi, P.Y., Lescar, J., Vasudevan, S.G., Luo, D., 2015. A crystal structure of the Dengue virus NS5 protein reveals a novel inter-domain interface essential for protein flexibility and virus replication. PLoS Pathog. 11, e1004682.

Zhou, Y., Ray, D., Zhao, Y., Dong, H., Ren, S., Li, Z., Guo, Y., Bernard, K.A., Shi, P.Y., Li, H., 2007. Structure and function of flavivirus NS5 methyltransferase. J. Virol. 81, 3891–3903.